Adaptive Visual Servo Control of Robot Manipulators via Composite Camera Inputs

Türker Şahin and Erkan Zergeroğlu
Department of Computer Engineering, Gebze Institute of Technology,
PK. 141, 41400 Gebze/Kocaeli-Turkey. e-mail: ezerger@bilmuh.gyte.edu.tr

Abstract: *This paper considers the problem of position control of robot manipulators via visual servoing in the presence of uncertainty associated with the robot dynamics and the vision system. Specifically, an adaptive controller is designed to compensate for the uncertainties associated with the mechanical parameters of the robot manipulator and the intrinsic parameters of the cameras. The 3d visual information is obtained from the composite inputs of two separate cameras placed in the robot work space. Despite the uncertainties associated with the camera system and robot dynamics the proposed adaptive controller achieves asymptotic end effector position tracking. A Lyapunov based approach is presented to prove the stability and boundedness of the closed loop system.*

1 Introduction

Non-contact sensing for control of robotic systems is essential for tracking and motion of manipulators in unstructured environments. A particularly important example to this is visual servoing, where information from vision sensors is used in the feedback loop to obtain the position information for the low level controllers. This work is based on a similar approach. Readers are referred to [1, 2] for more information on concurrent visual servoing.

Vision systems, used for robotic applications are mostly classified as a function of the number of vision sensors they use. They are either monocular visual servoing in which a single camera is utilized; or multi camera vision systems, where multiple cameras located in the work-space are used to collect the task specific information. The monocular systems are cost effective, but in nearly all 3D applications the work space depth information is lost. In fact it is sometimes even not possible for some multi-camera configurations to capture the scene depth, and hence careful camera calibration is necessary. However, it is usually difficult to obtain intrinsic camera parameters (i.e. the image center , magnification factors, and camera scaling factor), and the extrinsic cameras parameters (position and orientation of the camera within the work-space) exactly. For this reasons, a great deal of research has been applied to the camera calibration problem, but most solutions did not take the robot dynamics into account [3, 4, 5] and are limited to the kinematic level. It is crucial to incorporate the manipulator dynamics in the control loop for good performing visual servoing systems. However, so far such solutions have only been applied in monocular cases [6, 7, 8] and unfortunately most of related work constraints the problem to 2D case and ignores depth information. Recently, [9] presented an asymptotically stable position based visual feedback controller that can compensate the uncertainties of the homogenous transformation matrix between the task-space and the camera space, however the controller assumes that the intrinsic camera parameters are perfectly calibrated.

In this paper, the result given in [7] have been extended to 3D position servoing case via the use of multiple cameras. The controller proposed uses a similar transformation matrix as in [7] which premultiplies the composite camera calibration matrix so that the resultant matrix is positive definite and can be used to incorporate the camera parameters into the robot equation. A backstepping technique is then applied to achieve asymptotic end effector tracking. The controller requires the knowledge of position with respect to the base of the robotics manipulator for the cameras and still achieves asymptotic position tracking despite the uncertainties in the intrinsic the camera calibration parameters and the robot dynamics.

The following sections are organized in the following manner. In Section 2 the manipulator and the camera model used are presented. In Section 3 the control objective, controller development and stability analysis is presented, while the simulation results are presented in Section 4. Concluding remarks are summarized in Section 5.

2 Robot-Camera Model

A schematic representation of the robot-camera system configuration considered in this work is given in Figure 1. We assume that the cameras are located at fix points outside, but pointing towards the robot work-space such that: *i)* camera1 and camera2's image planes are parallel to $X_r - Y_r$ and $X_r - Z_r$ planes of motion of the robot respectively, and *ii)* both cameras can capture images throughout the entire robot work-space.

2.1 Robot Dynamics

The joint-space model for an three link, revolute, direct-drive, robot manipulator is assumed to be of the following form [12]

$$M(q)\ddot{q} + V_m(q,\dot{q})\dot{q} + G(q) + F(\dot{q}) = \tau \qquad (1)$$

where $q(t)$, $\dot{q}(t)$, $\ddot{q}(t) \in \mathbb{R}^3$ denote the link position, velocity, and acceleration vectors, respectively, $M(q) \in \mathbb{R}^{3\times3}$ represents the link inertia matrix, $V_m(q,\dot{q}) \in \mathbb{R}^{3\times3}$ represents

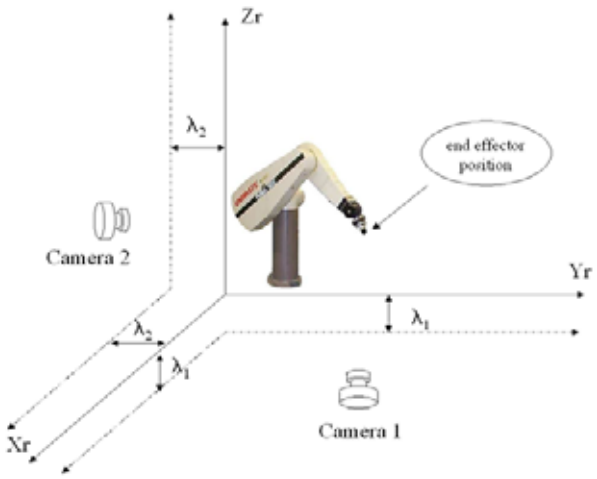

Figure 1: Placement of the Camera System with respect to Robot Coordinates

centripetal-Coriolis matrix, $G(q) \in \mathbb{R}^3$ represents the gravity effects, $F(\dot{q}) \in \mathbb{R}^3$ represents the friction effects, and $\tau(t) \in \mathbb{R}^3$ represents the torque input vector.

2.2 Composite Camera Model Development

Using the standard pin-hole model for a camera system, a point $x_r = \begin{bmatrix} x_1 & x_2 & x_3 \end{bmatrix}^T$ in a 3-D world frame, can be represented in terms of camera space coordinate frame as[10]

$$\begin{bmatrix} y_1 \\ y_2 \end{bmatrix} = \frac{f}{x_3} \begin{bmatrix} \beta_1 & 0 \\ 0 & \beta_2 \end{bmatrix} R(\theta) \left\{ \begin{bmatrix} x_1 \\ x_2 \end{bmatrix} - \begin{bmatrix} o_1 \\ o_2 \end{bmatrix} \right\} + \begin{bmatrix} c_1 \\ c_2 \end{bmatrix} \tag{2}$$

where $y = \begin{bmatrix} y_1 & y_2 \end{bmatrix}^T$ denotes the corresponding position vector in camera space, f is the focal length of the lens used, β_1, β_2 are the magnification factors of the camera, $R(\theta) \in \mathbb{R}^{2\times2}$ is the rotation matrix defined as

$$R(\theta) = \begin{bmatrix} \cos\theta & -\sin\theta \\ \sin\theta & \cos\theta \end{bmatrix} \tag{3}$$

with θ being the rotation angle of the camera, $O = \begin{bmatrix} o_1 & o_2 \end{bmatrix}^T$ is the position of the optical center of the camera with respect to the world coordinate frame and $C = \begin{bmatrix} c_1 & c_2 \end{bmatrix}^T$ denotes the image center which is defined as the frame buffer coordinates of the intersection of the optical axis with the image plane. Using the camera transformation given in (2) the camera space variables for the camera 1 of the system shown in Figure 1 is obtained for as follows

$$\begin{bmatrix} x_{c1} \\ y_{c1} \end{bmatrix} = \frac{1}{z_r + \lambda_1} H_1 R(\theta_1) \begin{bmatrix} x_r - o_{11} \\ y_r - o_{12} \end{bmatrix} + \begin{bmatrix} p_{11} \\ p_{12} \end{bmatrix} \tag{4}$$

where $H_1 \in \mathbb{R}^{2\times2}$ is defined as

$$H_1 = \begin{bmatrix} f_1\beta_{11} & 0 \\ 0 & f_1\beta_{12} \end{bmatrix}. \tag{5}$$

Similarly camera 2 variables are

$$\begin{bmatrix} x_{c2} \\ z_{c2} \end{bmatrix} = \frac{1}{y_r + \lambda_2} H_2 R(\theta_2) \begin{bmatrix} x_r - o_{21} \\ z_r - o_{22} \end{bmatrix} + \begin{bmatrix} p_{21} \\ p_{22} \end{bmatrix} \tag{6}$$

where H_1, H_2, $R(\theta_1)$, $R(\theta_2) \in \mathbb{R}^{2\times2}$ and $p_1 = \begin{bmatrix} p_{11} & p_{12} \end{bmatrix}^T$, $p_2 = \begin{bmatrix} p_{21} & p_{22} \end{bmatrix}^T \in \mathbb{R}^{2\times1}$ are constant but unknown camera parameters, λ_1,λ_2, o_{11}, o_{12}, o_{21}, o_{22} are positive constants representing the placement of the camera with respect to the origin of the robot world coordinate frame and are assumed to be known. Our first goal is to obtain a composite camera input from the two camera inputs placed in the work space that can lead us to obtain 3 dimensional position information (x_r, y_r, z_r) about the object in the work space as opposed to the normal 2-D projection using a standard camera. To this extend using the properties of the rotation matrix and the fact that H_2 is a diagonal matrix, z_{c2} defined in (6) can be written in the following form

$$z_{c2} = \gamma_1 \frac{z_r - o_{22}}{y_r + \lambda_2} + \gamma_2 x_{c2} + \gamma_3 \tag{7}$$

where the constant parameters γ_1, γ_2, $\gamma_3 \in \mathbb{R}$ are explicitly defined as

$$\begin{aligned} \gamma_1 &= \frac{f_2\beta_{22}}{\cos\theta_2},\ \gamma_2 = \frac{\beta_{22}\sin\theta_2}{\beta_{21}\cos\theta_2}, \\ \text{and } \gamma_3 &= p_{22} - p_{21}\frac{\beta_{22}\sin\theta_2}{\beta_{21}\cos\theta_2}. \end{aligned} \tag{8}$$

Based on (4) and (8) we find the composite camera input representation as follows

$$\begin{bmatrix} x_{c1} \\ y_{c1} \\ z_{c2} \end{bmatrix} = \overbrace{\begin{bmatrix} H_1R(\theta_1) & 0_{2\times1} \\ 0_{1\times2} & \gamma_1 \end{bmatrix}}^{\triangleq H\cdot R} \begin{bmatrix} \frac{x_r - o_{11}}{z_r + \lambda_1} \\ \frac{y_r - o_{12}}{z_r + \lambda_1} \\ \frac{z_r - o_{22}}{y_r + \lambda_2} \end{bmatrix} + \begin{bmatrix} p_{11} \\ p_{12} \\ \gamma_2 x_{c2} + \gamma_3 \end{bmatrix}. \tag{9}$$

For simplicity we defined the composite camera input vector $X_c = \begin{bmatrix} x_{c1} & y_{c1} & z_{c2} \end{bmatrix}^T$ and the off-setted cartesian vector $X_{\overline{R}} \in \mathbb{R}^3$ as

$$X_{\overline{R}} \triangleq \begin{bmatrix} \overline{x_r} \\ \overline{y_r} \\ \overline{z_r} \end{bmatrix} = \begin{bmatrix} x_r - o_{11} \\ y_r - o_{12} \\ z_r - o_{22} \end{bmatrix} \tag{10}$$

note that $X_{\overline{R}}$ can be calculated using the forward kinematics of the robot and the camera positioning values o_{11}, o_{12}, o_{22}. Taking the time derivative of (9) we obtain the following differential relationship between X_c and $X_{\overline{R}}$

$$\dot{X}_c = HRJ_c\dot{X}_{\overline{R}} + \begin{bmatrix} 0 \\ 0 \\ \gamma_2\dot{x}_{c2} \end{bmatrix} \tag{11}$$

where the composite camera image Jacobian, $J_c \in \mathbb{R}^{3\times3}$, is defined explicitly as

$$J_c = \begin{bmatrix} \frac{1}{(\overline{z_r}+\lambda_1+o_{22})} & 0 & -\frac{\overline{x_r}}{(\overline{z_r}+\lambda_1+o_{22})^2} \\ 0 & \frac{1}{(\overline{z_r}+\lambda_1+o_{22})} & -\frac{\overline{y_r}}{(\overline{z_r}+\lambda_1+o_{22})^2} \\ 0 & -\frac{\overline{z_r}}{(\overline{y_r}+\lambda_2+o_{12})^2} & \frac{1}{(\overline{y_r}+\lambda_2+o_{12})} \end{bmatrix}. \tag{12}$$

In (12) for the composite image Jacobian matrix, J_c, to be invertible the analysis requires that $\det(J_c)$ exists and is positive. This is supplied when $\lambda_2 + o_{12}$, and $\lambda_1 + o_{22}$ are both selected to be positive. Note that we restricted the motion of the manipulator to one quadrant to provide positive $\overline{y_r}$, and $\overline{z_r}$ values.

3 Control Formulation and Design

We will assume that a smooth, time varying, desired end effector trajectory generated in the camera space, denoted by $X_d(t) = \begin{bmatrix} x_d(t) & y_d(t) & z_d(t) \end{bmatrix}^T$ is constructed so that $X_d(t) \in C^2$. To provide a means of quantifying the position tracking control objective, we defined the position tracking error signal in camera space $e(t) \in \mathbb{R}^3$ as follows

$$e = X_d - X_c \tag{13}$$

taking time derivative of (13) and multiplying the resultant equation by

$$\begin{aligned} A &\triangleq \begin{bmatrix} A_1 & A_2 & 0 \\ A_3 & A_4 & 0 \\ 0 & 0 & A_5 \end{bmatrix} = (H\,R)^{-1} \\ &= \begin{bmatrix} \frac{\cos\theta_1}{f_1\beta_{11}} & \frac{\sin\theta_1}{f_1\beta_{12}} & 0 \\ -\frac{\sin\theta_1}{f_1\beta_{11}} & \frac{\cos\theta_1}{f_1\beta_{12}} & 0 \\ 0 & 0 & \frac{1}{\gamma_1} \end{bmatrix} \end{aligned} \tag{14}$$

to obtain

$$A\dot{e} = A\left\{\dot{X}_d - \begin{bmatrix} 0 \\ 0 \\ \gamma_2\dot{x}_{c2} \end{bmatrix}\right\} - J_c\,J\,\dot{q} \tag{15}$$

note that the forward kinematic relationship $\dot{X}_{\overline{R}} = J\dot{q}$ is utilized. Motivated by the subsequent stability analysis we pre-multiply both sides of (15) by the following transformation matrix

$$T = \begin{bmatrix} \frac{1}{A_1A_4 - A_3A_2} & \frac{A_3}{A_4} - \frac{A_2}{A_4(A_1A_4 - A_3A_2)} & 0 \\ 0 & 1 & 0 \\ 0 & 0 & 1 \end{bmatrix} \tag{16}$$

and obtain the following open loop dynamics for $e(t)$

$$Z\dot{e} = Z\left\{\dot{X}_d - \begin{bmatrix} 0 \\ 0 \\ \gamma_2\dot{x}_{c2} \end{bmatrix}\right\} - TJ_c\,J\,\dot{q} \tag{17}$$

where the constant matrix $Z \in \mathbb{R}^{3\times3}$ is defined as

$$Z = \begin{bmatrix} \frac{1+A_3^2}{A_4} & A_3 & 0 \\ A_3 & A_4 & 0 \\ 0 & 0 & A_5 \end{bmatrix} \tag{18}$$

and is positive definite when the rotation angles of the cameras satisfy $-\pi/2 < \theta_1, \theta_2 < \pi/2$. Following a backstepping like design procedure, we rewrite (17) in the following form;

$$Z\dot{e} = Z\left\{\dot{X}_d - \begin{bmatrix} 0 \\ 0 \\ \gamma_2\dot{x}_{c2} \end{bmatrix}\right\} - Tv + TJ_I\,\eta \tag{19}$$

where $J_I = J_c\,J$ is the image Jacobian and the auxiliary tracking like signal $\eta(t) \in \mathbb{R}^3$ is defined as

$$\eta = u - \dot{q} \tag{20}$$

with $u = J_I^{-1}v$. Using the definitions of (16) and (18) the open loop dynamics of (19) can be written in the following advantageous form

$$Z\dot{e} = \begin{bmatrix} \phi_4^{-1}(W_1\phi_1 - v_1) \\ W_2\phi_2 - v_2 \\ W_3\phi_3 - v_3 \end{bmatrix} + TJ_I\,\eta \tag{21}$$

where $W_1(.)$, $W_2(.)$, $W_3(.)$ are known regression matrices defined explicitly as

$$\begin{aligned} W_1 &= \begin{bmatrix} \dot{x}_d & \dot{y}_d & -v_2 \end{bmatrix}, \\ W_2 &= \begin{bmatrix} \dot{x}_d & \dot{y}_d \end{bmatrix}, \\ W_3 &= \begin{bmatrix} \dot{z}_d & \dot{x}_{c2} \end{bmatrix} \end{aligned} \tag{22}$$

and ϕ_1, ϕ_2, ϕ_3, ϕ_4 represents unknown constant parameter vectors with proper dimensions that are defined as

$$\begin{aligned} &\phi_1 = \begin{bmatrix} \frac{1+A_3^2}{A_4}\phi_4 & A_3\phi_4 & \frac{A_3\phi_4 - A_2}{A_4} \end{bmatrix}^T, \\ &\phi_2 = \begin{bmatrix} A_3 & A_4 \end{bmatrix}^T, \quad \phi_3 = \begin{bmatrix} \frac{1}{\gamma_1} & -\frac{\gamma_2}{\gamma_1} \end{bmatrix}^T, \\ &\phi_4 = A_1A_4 - A_2A_3 \end{aligned} \tag{23}$$

Based on the open-loop dynamics and the subsequent stability analysis the auxiliary internal control inputs are designed as follows

$$\begin{aligned} v_1 &= W_1\hat{\phi}_1 + k_1e_1,\, v_2 = W_2\hat{\phi}_2 + k_2e_2, \\ \text{and } v_3 &= W_3\hat{\phi}_3 + k_3e_3 \end{aligned} \tag{24}$$

where $e_i(t)$, $i = 1, 2, 3$ denote the elements of $e(t)$, k_1, k_2, k_3 are positive, scalar control gains and $\hat{\phi}_1(t) \in \mathbb{R}^3$, $\hat{\phi}_2(t) \in \mathbb{R}^2$, $\hat{\phi}_3(t) \in \mathbb{R}^2$are dynamic parameter estimates that are updated according to

$$\dot{\hat{\phi}}_1 = \Gamma_1W_1^Te_1,\, \dot{\hat{\phi}}_2 = \Gamma_2W_2^Te_2\,,\, \dot{\hat{\phi}}_3 = \Gamma_3W_3^Te_3 \tag{25}$$

where $\Gamma_1 \in \mathbb{R}^{3\times3}$, $\Gamma_2 \in \mathbb{R}^{2\times2}$and $\Gamma_3 \in \mathbb{R}^{2\times2}$ are diagonal, positive-definite, gain matrices. After substituting (24) into (21) we obtain the closed loop dynamics for $e(t)$ as follows

$$Z\dot{e} = \begin{bmatrix} \phi_4^{-1}(W_1\tilde{\phi}_1 - k_1e_1) \\ W_2\tilde{\phi}_2 - k_2e_2 \\ W_3\tilde{\phi}_3 - k_3e_3 \end{bmatrix} + TJ_I\,\eta. \tag{26}$$

The backstepping type control design also requires the dynamics for the auxiliary signal $\eta(t)$. For deriving this, we take the time derivative of (20) and pre-multiply the resultant equation by the inertia matrix to obtain

$$M\dot{\eta} = -V_m\eta - J_I^TT^Te - \tau + Y\theta \tag{27}$$

where $Y(.)$is a regression matrix containing the known/measurable terms and θ is the vector containing unknown but constant system parameter with proper dimensions and defined as

$$Y\theta = M\dot{u} + V_mu + F(\dot{q}) + G + J_I^TT^Te \tag{28}$$

note that the term $J_I^TT^Te$is injected to the dynamics to cancel the corresponding term in stability analysis.

Remark 1 *Based on the structure of (28) and standard adaptive controller design procedures, it is fairly easy to see that when the control torque input vector $\tau(t)$ with the parameter estimation vector $\hat{\theta}(t)$ are designed to have the following form*

$$\begin{aligned} \tau &= Y\hat{\theta} + K_\eta\eta, \\ \dot{\hat{\theta}} &= \Gamma_\theta\,Y^T\eta \end{aligned} \tag{29}$$

where $K_\eta \in R^{n\times n}$ is a constant, diagonal, positive definite, gain matrix and Γ_θ is a constant, diagonal, positive definite matrix with proper dimension, the tracking error can be driven to zero. However, as can be observed from (28) and (29) this approach requires the calculation of the time derivative of the auxiliary control input, $u(t)$, which in turns necessitates the calculations of the derivatives of the input $v(t)$ and the image Jacobian J_I on line. Thus, the implementation would require massive computations and hinders the analysis making the result unnecessarily complicated for practical purposes. In this work instead of using the forementioned standard adaptive controller approach, we will utilize a high gain controller that would treat the regression matrix multiplied by the uncertain parameter vector formulation as if it were a disturbance term and utilize a nonlinear damping argument to compensate for the unwanted effects of it. This method not only eases the implementation but also preserves the asymptotic stability result, as will be presented in the subsequent analysis.

Utilizing the fact that the system dynamics $Y\theta$ is bounded by a function of the form

$$\|Y\theta\| \leq \rho(\|x\|)\,\|x\| \tag{30}$$

with $x = \begin{bmatrix} e^T & \eta^T \end{bmatrix}$, the control torque input vector is designed to be:

$$\tau = k_n\rho(\|x\|)^2\eta + K_\eta\eta \tag{31}$$

where $K_\eta \in \mathbb{R}^{n\times n}$ is a constant, diagonal, positive definite, gain matrix. After substituting (31) in the (27) with the dynamics bounded by ω_R term, we obtain the closed loop dynamics for $\eta(t)$ as follows

$$M\dot{\eta} = -V_m\eta - J_I^T T^T e - K_\eta\eta - k_n\rho(\|x\|)^2\eta + Y\theta. \tag{32}$$

We now state the following Theorem:

Theorem 2 *The adaptive control law proposed by (24) with the update laws (25) and the control law of (31) ensure the global asymptotic end effector tracking in the sense that*

$$\lim_{t\to\infty} e(t) = 0 \tag{33}$$

provided that the damping gain obeys the following inequality

$$k_n \geq \frac{1}{\min(\lambda_{\min}\{K_\eta\}, \min(\phi_4^{-1}k_1, k_2, k_3))} \tag{34}$$

and the camera orientations satisfy the following condition

$$-\pi/2 < \theta_i < \pi/2, \quad i = 1, 2\,. \tag{35}$$

Proof : We begin our proof by introducing the following non-negative scalar function

$$\begin{aligned} V &= \frac{1}{2}e^T Z e + \frac{1}{2}\eta^T M\eta + \frac{1}{2}\phi_4^{-1}\tilde{\phi}_1^T\Gamma_1^{-1}\tilde{\phi}_1 \\ &\quad + \frac{1}{2}\tilde{\phi}_2^T\Gamma_2^{-1}\tilde{\phi}_2 + \frac{1}{2}\tilde{\phi}_3^T\Gamma_3^{-1}\tilde{\phi}_3. \end{aligned} \tag{36}$$

Taking the time derivative of this expression, then inserting the closed loop dynamics from (26) and (32), applying the well known skew symmetric relationship between the inertia and centripetal-Coriolis matrices and making the appropriate eliminations, we obtain,

$$\begin{aligned} \dot{V} &= -\phi_4^{-1}k_1e_1^2 - k_2e_2^2 - k_3e_3^2 \\ &\quad -\eta^T\left[(K_\eta\eta + k_n\rho(\|x\|)^2\eta) + \rho(\|x\|)\,\|x\|\right]. \end{aligned} \tag{37}$$

Completing the squares of terms in the brackets of (37), we can further upperbound this expression to have the following form

$$\dot{V} \leq -\beta\,\|x\|^2\,. \tag{38}$$

where $\beta = \min\left\{\lambda_{\min}\{K_\eta\}, \min(\phi_4^{-1}k_1, k_2, k_3)\right\} - \frac{1}{k_n}$ and the definition (30) has been applied for x. From (36) and (38) provided that (34) is satisfied, we can conclude that $V(t) \in \mathcal{L}_\infty$; hence, $e(t)$, $\eta(t)$, $\tilde{\phi}_1(t)$, $\tilde{\phi}_2(t)$, and $\tilde{\phi}_3(t) \in \mathcal{L}_\infty$. Standard signal chasing arguments can be used to prove that all system and controller signals defined (31), (24) and (25) are bounded. Due to the boundedness of $\dot{e}(t)$, we can conclude that $e(t)$ is uniformly continuous. In addition, it is straightforward to use (38) to illustrate that $e(t) \in \mathcal{L}_2$. At this point from direct application of Barbalat's Lemma [11] we conclude (33) □

4 Simulation Results

To illustrate the performance of the proposed controller we selected a 3 dof robot manipulator with

$$\begin{aligned} M &= \begin{bmatrix} M_{11} & 0 & 0 \\ 0 & M_{22} & M_{23} \\ 0 & M_{32} & M_{33} \end{bmatrix}, \\ V_m &= \begin{bmatrix} V_{11} & 0 & 0 \\ 0 & V_{22} & V_{23} \\ 0 & V_{32} & 0 \end{bmatrix}, \quad G = \begin{bmatrix} 0 \\ G_2 \\ G_3 \end{bmatrix} \end{aligned} \tag{39}$$

where the entries are formulated as

$$\begin{aligned} M_{11} = {} & m_3(l_2\cos(q_2) + l_{c3}\cos(q_2+q_3))^2 \\ & + m_2 l_{c2}^2\cos^2(q_2) + A_2\sin^2(q_2) \\ & + A_3\sin^2(q_2+q_3) + E_1 \\ & + E_3\cos^2(q_2) + E_3\cos^2(q_2+q_3) \\ M_{22} = {} & m_2 l_{c2}^2\sin^2(q_2) + l_2 + l_3 \\ & + m_3(l_2^2 + l_{c3}^2 + 2l_2 l_{c3}\cos(q_3)) \\ M_{23} = {} & M_{32} = m_3(l_{c3}^2 + l_2 l_{c3}\cos(q_3)) + l_3 \\ M_{33} = {} & m_3 l_{c3} + l_3 \end{aligned} \tag{40}$$

$$\begin{aligned} V_{11} = {} & -m_3 l_2 l_{c3}(\dot{q}_2+\dot{q}_3)\sin(q_2+q_3)\cos(q_2) \\ & - m_3 l_2 l_{c3}\dot{q}_2\sin(q_2)\cos(q_2+q_3) \\ & - (m_2 l_{c2}^2 + m_3 l_2^2 + E_3)\dot{q}_2\sin(q_2)\cos(q_2) \\ & - E_3(\dot{q}_2+\dot{q}_3)\sin(q_2+q_3)\cos(q_2+q_3) \\ & - m_3 l_{c3}^2(\dot{q}_2+\dot{q}_3)\sin(q_2+q_3)\cos(q_2+q_3) \\ & + A_2\dot{q}_2\sin(q_2)\cos(q_2) \\ & + A_3(\dot{q}_2+\dot{q}_3)\sin(q_2+q_3)\cos(q_2+q_3) \\ V_{22} = {} & -m_3 l_2 l_{c3}\dot{q}_3\sin(q_3) \\ & + m_2 l_{c2}^2\dot{q}_2\sin(q_2)\cos(q_2) \\ V_{23} = {} & V_{32} = -0.5 m_3 l_2 l_{c3}\dot{q}_3\sin(q_3) \end{aligned} \tag{41}$$

$$\begin{aligned} G_2 = {} & 9.8(m_2 l_{c2} + m_3 l_2)\cos(q_2) \\ & + 9.8 m_3 l_{c3}\cos(q_2+q_3) \\ G_3 = {} & 9.8 m_3 l_{c3}\cos(q_2+q_3) \end{aligned} \tag{42}$$

In these matrices the coefficients of the entries are the lengths of the manipulator links $l_1 = 0.5$, $l_2 = 0.4$, $l_3 = 0.4$ in metres, the masses of the links $m_1 = 4, m_2 = 3$ and

$m_2 = 3$ in kg, distances of the link joints $l_{c2} = 0.2$, $l_{c3} = 0.2$ in metres, and the cylindrical link radius $R = 0.05$. The torque limits are $\tau_i = \pm 50$ and the cylindrical link inertial parameters are obtained by $E_1 = m_1 R^2/2$, $E_i = m_i R^2/12$, $A_i = m_i R^2/2$ and $l_i = m_i R^2/12$, where $i = 2, 3$ for the robot links.

The desired position trajectory in the composite camera space is selected as

$$X_d(t) = \begin{bmatrix} 465 + 20\sin(\frac{\pi}{6}t + \frac{\pi}{12}) \\ 490 + 25\sin(\frac{\pi}{6}t + \frac{5\pi}{12}) \\ 480 + 20\sin(\frac{\pi}{6}t + \frac{5\pi}{12}) \end{bmatrix} \quad (43)$$

with all components in pixels. The overall system enables accurate tracking of objects having similar initial positions and rotational terms in the same amplitude range, which ensure that the singularities of the robot arm is not forced. The composite camera output is in figure 2 to reflect this property. The selected internal controller gain matrix is:

$$K \triangleq diag\{ \ k_1 \quad k_2 \quad k_3 \ \} = diag\{ \ 3 \quad 1.5 \quad 2 \ \} \quad (44)$$

while the applied adaptation term parameters are as below:

$$\begin{aligned} \Gamma_1 &= diag\{ \ 0.5 \quad 0.0001 \quad 0.01 \ \}, \quad (45) \\ \Gamma_2 &= diag\{ \ 0.001 \quad 0.005 \ \}, \\ \Gamma_3 &= diag\{ \ 0.00005 \quad 0.00001 \ \}. \end{aligned}$$

Similarly the outer loop control has the control gain matrix and the damping gain coefficient selected as:

$$\begin{aligned} K_\eta = diag\{ \ 50 \quad 75 \quad 25 \ \}, \\ k_n = 25. \end{aligned} \quad (46)$$

The above parameter selections enable accurate position tracking performance with acceptable error terms as depicted in Figure 3. The applied torque output is in Figure 4, while Figure 5 is on the parameter estimates for the inner loop.

5 Conclusion

We have presented a nonlinear, adaptive, 3-D end effector position tracking controllers for a vision based system composed of 2 fixed cameras The proposed controller achieves asymptotic end effector tracking despite the presence of uncertainties in the intrinsic camera parameters of both vision sensors and the robot dynamics. This result was obtained by applying a novel approach to compose the camera inputs and form the 3 dimensional end effector position information in camera space and using a backstepping design scheme. Considering the similarities between the controller design procedures our controller might be considered as the 3-D extension of [7] with the use of multiple cameras. Unfortunately our controller requires the calculation of second derivative of the redundant camera measurements.

References

[1] G.D. Hager and S. Hutchinson (guest editors), Special Section on Vision-Based Control of Robot Manipulators, *IEEE Trans. Robotics and Automation*, Vol. 12, No. 5, Oct. 1996.

[2] B. Nelson and N. Papanikolopoulos (guest editors), Special Issue of Visual Servoing, *IEEE Robotics and Automation Mag.*, Vol. 5, No. 4, Dec. 1998.

[3] F. Miyazaki and Y. Masutani, "Robustness of Sensory Feedback Control Based on Imperfect Jacobian", *Robotics Research: The Fifth Int. Symp.*, pp. 201-208, H. Miura and S. Arimoto, Eds., Cambridge, MA: MIT Press, 1990.

[4] G.D. Hager, W.C. Chang, and A.S. Morse, "Robot Hand-Eye Coordination Based on Stereo Vision", *IEEE Control Systems Mag.*, Vol. 15, No. 1, pp. 30-39, Feb. 1995.

[5] B. H. Yoshima and P. K. Allen, "Active, uncalibrated Visual Servoing", *in Proc. IEEE Int. Conf. Robotics and Automation*, pp 156-161, 1994.

[6] R. Kelly, "Robust Asymptotically Stable Visual Servoing of Planar Robots", *IEEE Trans. Robotics and Automation,* Vol 12, No. 5, pp.759-766, 1996.

[7] E. Zergeroglu, D. Dawson, M.S. de Queiroz, and A. Behal, "Vision-Based Nonlinear Tracking Controllers with Uncertain Robot-Camera Parameters ", *IEEE/ASME Transactions on Mechatronics,* Vol. 6, No 3, pp 322-337, September 2001.

[8] E. Zergeroglu, D. M. Dawson, M. S. de Queiroz, and P. Setlur, "Robust Visual-Servo Control of Planar Robot Manipulators in the presence of uncertainty", *Journal of Robotic Systems*, Volume 20, Issue 2, pp. 93-106, Feb. 2003.

[9] Y. Shen, D. Sun, Y. Lui, K. Li, "Asymptotic Trajectory Tracking of Manipulators Using Uncalibrated Visual Feedback", *IEEE/ASME Transactions on Mechatronics,* Vol. 8, No 1, pp 87-98, March 2003.

[10] R.K. Lenz and R.Y. Tsai, "Techniques for Calibration of the Scale Factor and Image Center for High Accuracy 3-D Machine Vision Metrology", *IEEE Trans. Pattern Analysis and Machine Intelligence,* Vol. 10, No. 5, Sept. 1988.

[11] J.J. Slotine and W. Li, *Applied Nonlinear Control*, Englewood Cliff, NJ: Prentice Hall, 1991.

[12] M.W. Spong and M. Vidyasagar, *Robot Dynamics and Control*, New York, NY: John Wiley and Sons, 1989.

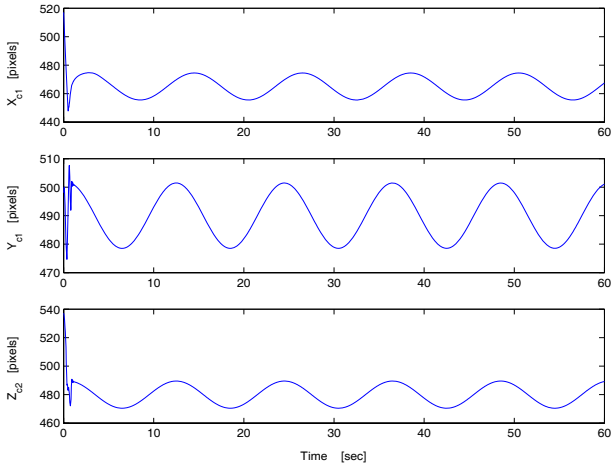

Figure 2: The End Effector Trajectory as seen from the Composite Camera During the Simulation

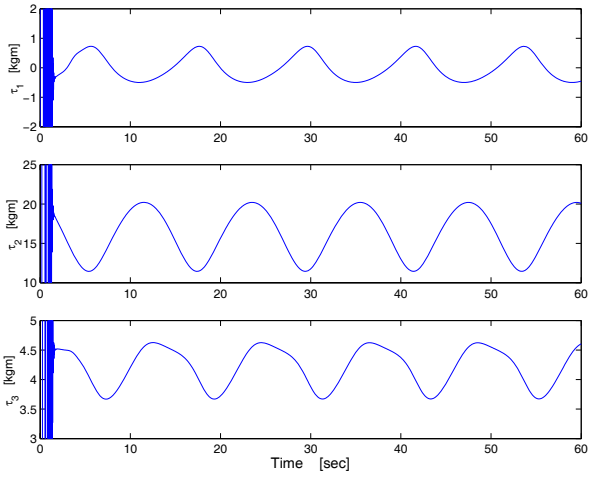

Figure 4: Input Control Torques

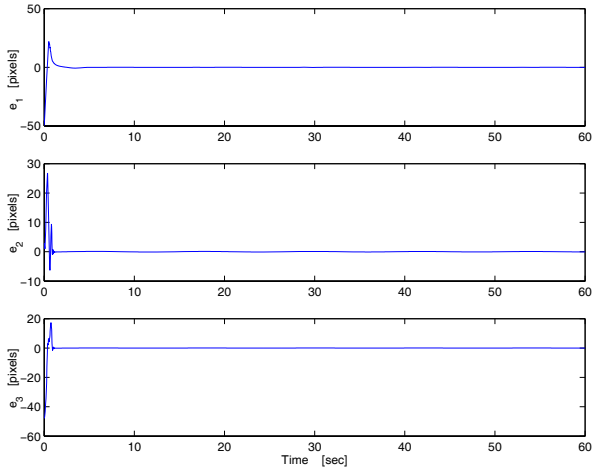

Figure 3: Tracking Error Terms

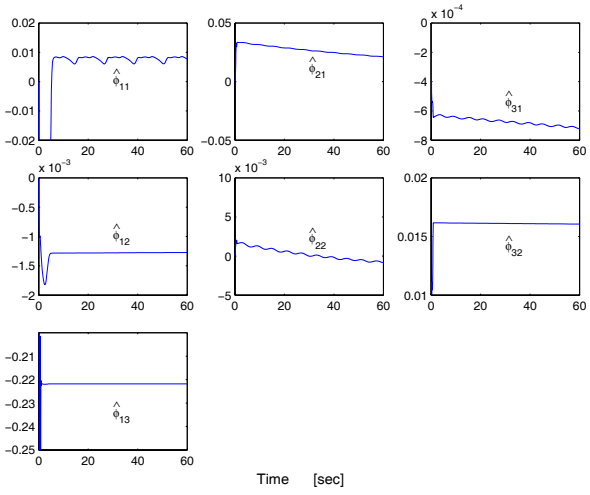

Figure 5: Estimates for the Uncertain Parameters of the Cameras